

Article

Thermo-responsive polymer micelles as potential nano-sized cancerostatics

Richard Laga, Olga Janoušková, Karel Ulbrich, Robert Pola, Jana Blažková, Sergey K. Filippov, Tomas Etrych, and Michal Pechar

Biomacromolecules, **Just Accepted Manuscript** • DOI: 10.1021/acs.biomac.5b00764 • Publication Date (Web): 08 Jul 2015

Downloaded from <http://pubs.acs.org> on July 12, 2015

Just Accepted

“Just Accepted” manuscripts have been peer-reviewed and accepted for publication. They are posted online prior to technical editing, formatting for publication and author proofing. The American Chemical Society provides “Just Accepted” as a free service to the research community to expedite the dissemination of scientific material as soon as possible after acceptance. “Just Accepted” manuscripts appear in full in PDF format accompanied by an HTML abstract. “Just Accepted” manuscripts have been fully peer reviewed, but should not be considered the official version of record. They are accessible to all readers and citable by the Digital Object Identifier (DOI®). “Just Accepted” is an optional service offered to authors. Therefore, the “Just Accepted” Web site may not include all articles that will be published in the journal. After a manuscript is technically edited and formatted, it will be removed from the “Just Accepted” Web site and published as an ASAP article. Note that technical editing may introduce minor changes to the manuscript text and/or graphics which could affect content, and all legal disclaimers and ethical guidelines that apply to the journal pertain. ACS cannot be held responsible for errors or consequences arising from the use of information contained in these “Just Accepted” manuscripts.



Thermo-responsive polymer micelles as potential nano-sized cancerostatics

Richard Laga, Olga Janoušková, Karel Ulbrich, Robert Pola, Jana Blažková, Sergey K.*

Filippov, Tomáš Etrych and Michal Pechar

Institute of Macromolecular Chemistry Academy of Sciences of the Czech Republic, v.v.i,

Department of Biomedical Polymers, Heyrovský sq. 2, 162 06 Prague, Czech Republic

Keywords

RAFT polymerization; polymer therapeutics; thermo-responsive micelles; light scattering; laser scanning confocal microscopy; cancer therapy

Abstract

An effective chemotherapy for neoplastic diseases requires the use of drugs that can reach the site of action at a therapeutically efficacious concentration and maintain it at a constant level over a sufficient period of time with minimal side effects. Currently, conjugates of high-molecular-weight hydrophilic polymers or biocompatible nanoparticles with stimuli-releasable anti-cancer drugs are considered to be some of the most promising systems capable of fulfilling these criteria. In this work, conjugates of thermo-responsive di-block copolymers with the covalently bound cancerostatic drug pirarubicin (PIR) were synthesized as a reversible micelle-forming drug delivery system combining the benefits of the above mentioned carriers. The di-block copolymer carriers were composed of hydrophilic poly[*N*-(2-

1
2
3 hydroxypropyl)methacrylamide]-based block containing a small amount (~ 5 mol. %) of
4
5 comonomer units with reactive hydrazide groups and a thermo-responsive poly[2-(2-
6
7 methoxyethoxy)ethyl methacrylate] block. PIR was attached to the hydrophilic block of the
8
9 copolymer through the pH-sensitive hydrazone bond designed to be stable in the blood stream at
10
11 pH 7.4 but to be degraded in the intratumoral/intracellular environment at pH 5 - 6. The
12
13 temperature-induced conformation change of the thermo-responsive block (coil-globule
14
15 transition), followed by self-assembly of the copolymer into a micellar structure, was controlled
16
17 by the thermo-responsive block length and PIR content. The cytotoxicity and intracellular
18
19 transport of the conjugates as well as the release of PIR from the conjugates inside the cells,
20
21 followed by its accumulation in the cell nuclei, were evaluated *in vitro* using human colon
22
23 adenocarcinoma (DLD-1) cell lines. It was demonstrated that the studied conjugates have a great
24
25 potential to become efficacious *in vivo* pharmaceuticals.
26
27
28
29
30
31

32 **Introduction**

33
34
35 Currently, neoplastic diseases, together with cardiovascular diseases, two of the most common
36
37 fatal illnesses, represent a serious health problem in patient populations ¹. The treatment of
38
39 neoplastic diseases using conventional chemotherapeutics – low-molecular-weight compounds
40
41 with cancerostatic effects – may lead to the suppression or even a complete cure of the disease;
42
43 however, such treatment is usually associated with particular side effects. These side effects are
44
45 mainly the result of ineffective localization of a cytotoxic drug in a tumor, often leading to the
46
47 irreversible damage to healthy cells and tissue. Moreover, the treatment using low-molecular-
48
49 weight chemotherapeutics commonly requires relatively frequent dosing as the drug
50
51 concentration at the site of action rapidly decreases due to rapid blood clearance, glomerular
52
53 filtration and drug elimination.
54
55
56
57
58
59
60

1
2
3 The chemotherapeutic strategy using conjugates of high-molecular-weight (HMW) synthetic
4 hydrophilic polymer carriers with covalently linked drugs is considered to be one of the most
5 effective ways to prolong blood clearance and reliably reduce unwanted side effects². Based on
6 the differences in the endothelial permeability of the healthy and the malignant tissues, such
7 conjugates are able to deliver the drug preferentially to the tumor tissue without significantly
8 affecting the healthy cells³⁻⁵. Furthermore, properly chosen stimuli-sensitive biodegradable
9 linker inserted between the polymer backbone and the drug may ensure the conjugate stability in
10 the circulation and a long-lasting release of the drug directly inside the tumor or the cancer cells
11
12
13
14
15
16
17
18
19
20
21
22
23
24
25
26
27
28
29
30
31
32
33
34
35
36
37
38
39
40
41
42
43
44
45
46
47
48
49
50
51
52
53
54
55
56
57
58
59
60

It was shown that the level of the passive accumulation of the conjugates in the solid tumors due to the enhanced permeability and retention (EPR) effect depends to a large extent on the size or molecular weight of the polymer carrier⁹. Current synthetic procedures enable the preparation of polymer-drug conjugates with a broad range of molecular weights and sizes of polymer coils^{10,11}. Unfortunately, the elimination of such conjugates from the body after delivering the drug (one of the basic requirements for drug delivery carriers) is limited by the molecular weight, e.g., for *N*-(2-hydroxypropyl)methacrylamide (HPMA)-based polymers not exceeding 50 kDa, unless they are biodegradable⁹. The size of such macromolecules is rather small to achieve an efficient EPR effect and the synthesis of biodegradable HMW conjugates is not a simple task. HMW drug carriers based on polymer micelles prepared by self-assembly of smaller amphiphilic copolymers (excretable in a form of unimer) offer a beneficial solution to this problem. Such nano-sized materials are usually prepared from block or graft copolymers consisting of hydrophilic and hydrophobic chains of various lengths and compositions. Copolymers based on non-reactive poly(ethylene glycol)/poly(L-lactide), poly(ethylene glycol)/poly(γ -benzyl-L-glutamate) or

1
2
3 poly(ethylene glycol)/poly(propylene glycol) are among the most examined ones¹²⁻¹⁴. These
4
5 copolymers have been described as carriers of hydrophobic drugs which, in most cases, were
6
7 non-covalently (hydrophobic interaction) incorporated into the hydrophobic core of the micelles
8
9 through the self-assembly process. In spite of the structural and morphological variability of
10
11 these materials, the relatively difficult preparation of the defined micelles, together with their
12
13 tendency to aggregate, lower drug loading and complicated long-term storage, limits their
14
15 clinical application.
16
17
18

19
20 A suitable alternative to the above mentioned polymer micelles might be reversible
21
22 temperature-sensitive micelles comprising a combination of hydrophilic and thermo-responsive
23
24 block copolymers. The thermo-responsive polymers are distinct in their ability to reversibly
25
26 change the chain morphology – from the random coil conformation (soluble form), to the
27
28 condensed globule (insoluble form) – depending on the temperature of the incubation media.
29
30 From the biomedical application point of view, the coil-globule transition temperature (T_{tr}) of the
31
32 thermo-responsive polymer chain should be slightly below physiological temperature (37 °C) to
33
34 allow for the easy dissolution of the block copolymer in laboratory conditions and spontaneous
35
36 formation of the defined micelles immediately before (by heating up the solution to 37 °C) or
37
38 upon sample administration. Copolymers based on poly(*N*-isopropylacrylamide)
39
40 (poly(NIPAAm))^{15, 16}, poly(2-isopropyl-2-oxazoline) (poly(IPOX))^{17, 18} and elastin side-chain
41
42 polymers¹⁹ are examples of the most commonly studied materials meeting these requirements,
43
44 although the individual polymers exhibit particular pitfalls that might prevent their possible
45
46 application in the clinics. These limitations are the relatively strong dependence of the T_{tr} on the
47
48 degree of polymerization (poly(NIPAAm)), the concentration (elastin-based polymers) and the
49
50
51
52
53
54
55
56
57
58
59
60

1
2
3 relatively complex preparation technique that does not allow the synthesis of HMW uniform
4
5 polymers (poly(IPOX))^{20, 21}.
6
7

8 Considering the facts mentioned above, copolymers based on the poly[2-(2-
9 methoxyethoxy)ethyl methacrylate] (poly(DEGMA)) seemed to be suitable candidates for the
10 proposed purposes as they fully meet the criteria for the biomedical application including the
11 nontoxicity, biocompatibility and transition temperature requirements ($T_{tr} \approx 24 - 28 \text{ }^\circ\text{C}$) and do
12 not show the limitations observed in the case of the above mentioned materials^{20, 22, 23}. In this
13 study, we used the unique combination of thermo-responsive poly(DEGMA) with the highly
14 hydrophilic *N*-(2-hydroxypropyl)methacrylamide copolymers (poly(HPMA)), which have often
15 been applied as carriers for drug, protein or gene delivery²⁴⁻²⁶. The initial di-block copolymer
16 precursors with various lengths of the thermo-responsive poly(DEGMA) blocks were
17 synthesized by the reversible addition-fragmentation chain-transfer (RAFT) polymerization
18 technique, enabling the preparation of the precisely defined materials. The poly(HPMA) block
19 contained ~5 mol. % of comonomer units with hydrazide groups intended for the attachment of
20 the cancerostatic drug pirarubicin (PIR). PIR was bound to the hydrophilic blocks of the
21 copolymers through the pH-sensitive hydrazone bond, which proved to be stable in the blood
22 stream at pH 7.4 but to undergo pH-sensitive hydrolysis in the intratumoral and intracellular
23 environment at pH below 6.5. The influence of the physicochemical parameters of the conjugates
24 on their in vitro biological behavior was investigated using the colorectal adenocarcinoma DLD-
25 1 cell lines. It was demonstrated that the studied conjugates effectively penetrated the cell
26 membranes of the cancer cells and released PIR inside the cells, which resulted in changed cell
27 morphology and damaged mutual intracellular connections, both indicating approaching cell
28 death.
29
30
31
32
33
34
35
36
37
38
39
40
41
42
43
44
45
46
47
48
49
50
51
52
53
54
55
56
57
58
59
60

Experimental section

Materials

(*RS*)-1-Aminopropan-2-ol, 6-aminohexanoic acid (Ahx), 2,2'-azobis(2-methylpropionitrile) (AIBN), 2-cyano-2-propyl benzodithioate (CPB), 4-cyano-4-thiobenzoylsulfanylpentanoic acid (CTP), *N,N'*-dicyclohexylcarbodiimide (DCC), *N,N'*-dimethylacetamide (DMA), dimethyl sulfoxide (DMSO), 1,4-dioxan, methacryloyl chloride, 2-(2-methoxyethoxy)ethyl methacrylate (DEGMA), *tert*-butanol, *tert*-butyl carbazate, triisopropylsilane (TIPS), trifluoroacetic acid (TFA), 2,4,6-trinitrobenzenesulfonic acid solution (1 M in H₂O) were purchased from Sigma-Aldrich (Sigma-Aldrich spol. s r.o., Czech Republic). Pirarubicin (PIR) was obtained from Meiji Seika Pharma Co., Ltd. (Japan), and DY-676 NHS-ester was purchased from Dyomics GmbH (Germany). All other chemicals and solvents were of analytical grade. Solvents were dried and purified by conventional procedures and distilled before use.

The EL-4 and DLD1 cell lines were obtained from ATCC (LGC Standards Sp. z o.o., Poland). Dulbecco's Modified Eagle Medium (DMEM) and RPMI-1640 media, Alamar Blue cell viability reagent and Hoechst 33342 were purchased from Life Technology (Life Technologies Czech Republic s.r.o., Czech Republic).

Size-exclusion chromatography (SEC)

The molecular weights and polydispersities of the polymers and polymer-PIR conjugates were determined by SEC on a Shimadzu HPLC system equipped with UV–VIS diode array detector (Shimadzu, Japan), refractive index Optilab-rEX, and multiangle light scattering DAWN EOS detectors (Wyatt Technology Corp., Santa Barbara, CA). TSK-Gel SuperAW3000 and SuperAW4000 columns connected in series and 80 % methanol / 20 % sodium acetate buffer (0.3 M, pH 6.5) as an eluent at a flow rate of 0.6 mL/min were used in all experiments. A method

1
2
3 based on the known total injected mass with an assumption of 100 % recovery was used for the
4
5 calculation of the molecular weights from light scattering data. The number- and weight-average
6
7 molecular weights for the polymer precursors and the polymer-PIR conjugates are summarized
8
9 in Table 1 and Table 2, respectively.
10
11

12 13 *UV/VIS spectrophotometry*

14
15 The spectrophotometric analyses were carried out in quartz glass cuvettes on a UV/VIS
16
17 spectrophotometer Helios Alpha (Thermospectronic, UK). The content of dithiobenzoate (DTB)
18
19 end groups in the polymers were determined at 302 nm in methanol using the molar absorption
20
21 coefficient $\epsilon^{\text{DTB}} = 12,100 \text{ L/mol}\cdot\text{cm}$. The content of hydrazide groups in the polymer precursors
22
23 was determined using a modified TNBSA assay as described earlier.²⁷ The results are
24
25 summarized in Table 1. The determination of the PIR content in the polymer-PIR conjugates
26
27 (without fluorophore) was performed at 488 nm in methanol using the molar absorption
28
29 coefficient $\epsilon^{\text{PIR}} = 11,300 \text{ L/mol}\cdot\text{cm}$. The PIR contents are summarized in Table 2. The content of
30
31 carbonylthiazolidine-2-thione (TT) reactive groups in the polymer precursor was determined at
32
33 305 nm using the molar absorption coefficient $\epsilon^{\text{TT}} = 10,300 \text{ L/mol}\cdot\text{cm}$.
34
35
36
37
38
39

40 41 *Dynamic light scattering (DLS)*

42
43 The hydrodynamic radii (RH) and scattering intensities (IS) of the polymer precursors and
44
45 polymer conjugates were measured by the DLS technique at a scattering angle $\theta = 173^\circ$ using a
46
47 Nano-ZS instrument (Model ZEN3600, Malvern Instruments, UK) equipped with a 632.8 nm
48
49 laser. The temperature measurements were performed to investigate the self-assembly of
50
51 polymer coils to polymer micelles in the temperature range 20 - 50 °C (in 1 °C increments) in
52
53 PBS (1.0 mg/mL, pH 7.4) solutions. At each step, measurements were performed after reaching
54
55 the steady state conditions, which typically required approximately 10 min. For the evaluation of
56
57
58
59
60

1
2
3 the dynamic light scattering data, the DTS(Nano) program was used. The mean of at least three
4
5 independent measurements was calculated. The transition temperature (T_{tr}) characterizing the
6
7 polymer chain conformation changes was evaluated from the temperature dependence of the
8
9 hydrodynamic diameter (D_H); the T_{tr} value was determined from the intersection point of two
10
11 lines formed by the linear regression of a lower horizontal asymptote and a vertical section of the
12
13 S-shaped curve (sigmoidal curve) fit. The T_{tr} values for the polymer precursors and the polymer-
14
15 PIR conjugates are summarized in Table 1 and Table 2, respectively.
16
17
18
19

20 21 *PIR release assays*

22
23 The release of PIR from the polymer-PIR conjugates was measured in aqueous solutions at 37
24
25 °C at two different pH values using a monochromator-based multi-mode microplate reader
26
27 Synergy H1 (BioTek, USA). Specifically, the polymer conjugates ($c = 2.5$ mg/mL) were
28
29 dissolved in 0.15 M PBS (pH 5.5 or 7.4), heated up to 37 °C and kept at this temperature for the
30
31 duration of the analysis. In the selected time intervals, the aliquots (140 μ L) were loaded on the
32
33 preheated PD SpinTrap G-25 columns (GE Healthcare, UK) and centrifuged at 37 °C for 2
34
35 minutes at $800 \times g$. Subsequently, the absorbances of the collected polymer fractions were
36
37 measured in 96-well plates at 486 nm. The PIR release from the polymer-PIR conjugates was
38
39 plotted as the relative decrease of amount of polymer-bound pirarubicin over time. An
40
41 absorbance of the appropriate polymer-PIR conjugate measured immediately upon its dissolution
42
43 and subsequent centrifugation was used as an initial value ($A(t_0)$).
44
45
46
47
48

49 The stabilities of the polymer-PIR conjugates in the buffers modeling both extracellular and
50
51 intracellular environments were also evaluated using a SEC column on the Shimadzu HPLC
52
53 system (see above). Specifically, the polymer conjugates ($c = 1.0$ mg/mL) were dissolved in 0.15
54
55 M PBS (pH 5.5 or 7.4), heated up to 37 °C and kept at this temperature for the duration of the
56
57
58
59
60

1
2
3 analysis. At selected time intervals, the aliquots (20 μL) were loaded on the TSK-Gel
4
5 SuperAW3000/4000 column and eluted using the 80 % methanol / 20 % sodium acetate buffer
6
7 (0.3 M, pH 6.5) mixture. The relative amount of the polymer-bound PIR was evaluated from the
8
9 polymer peak area recorded by the UV–VIS detector at 486 nm. The release of PIR from the
10
11 conjugates was plotted as a change of the polymer-bound PIR concentration over time.
12
13
14

15 16 *Isothermal Titration Calorimetry (ITC)*

17
18 The critical micellar concentration (CMC) values were determined by an isothermal titration
19
20 microcalorimeter MicroCal iTC200. The ITC experiments were performed using either 20
21
22 injections of the polymer solution in PBS buffer above the T_{tr} into PBS buffer (a constant
23
24 titration volume of 2 μL ; 180 s intervals). The thermograms were recorded and analyzed using
25
26 Origin 7 software.
27
28
29

30 31 *Cell line cultures*

32
33 EL-4 murine T-cell lymphoma cell line was cultured in DMEM supplemented with heat
34
35 inactivated 10 % fetal calf serum (FCS), penicillin (100 U/mL) and streptomycin (100 $\mu\text{g}/\text{mL}$).
36
37 The DLD-1 human colorectal adenocarcinoma cell line was cultured in RPMI-1640 medium
38
39 with heat inactivated 10 % FCS, penicillin (100 $\mu\text{g}/\text{mL}$) and streptomycin (100 $\mu\text{g}/\text{mL}$).
40
41
42
43

44 45 *In vitro cell viability assay*

46
47 DLD1 (5×10^4) or EL4 cells (15×10^4) were seeded in 100 μL media into 96-well flat-bottom
48
49 plates 24 h before the addition of the polymer-PIR conjugates or free PIR. The polymer-PIR
50
51 conjugate stock solutions (5 mg/mL in PBS) were diluted with PBS to concentrations ranging
52
53 from 0.2 to 200 $\mu\text{g}/\text{mL}$; PIR was firstly dissolved in DMSO (10 mg/mL) and then diluted with
54
55 PBS to 0.01 – 100 $\mu\text{g}/\text{mL}$. Thereafter, 10 μL of the polymer-PIR conjugates or PIR were added
56
57
58
59
60

1
2
3 to the cells and the cells were cultured for 72 h in 5 % CO₂ atmosphere at 37°C. Then, 10 µL of
4
5 Alamar Blue cell viability reagent was added to each well and allowed to incubate for 4 h at 37
6
7 °C. In viable cells, the active component of the Alamar Blue reagent – resazurin – was reduced
8
9 to the highly fluorescent compound resorufin. The fluorescence of resorufin was detected using
10
11 the Synergy Neo plate reader (BioTek, USA) at 570/610 nm (excitation/emission). The cells
12
13 cultured in a medium without Alamar Blue were used as negative controls. Three wells were
14
15 used for each concentration. The assay was repeated three times independently. Statistical
16
17 analysis for one-way ANOVA was performed using the GraphPad Prism Software. The IC₅₀
18
19 values for the polymer-PIR conjugates and free PIR are summarized in Table 3.
20
21
22
23
24

25 *Internalization of fluorescently labeled polymer-PIR conjugates*

26
27
28 DLD1 cells were cultured for 24 h in 5 % CO₂ atmosphere at 37°C on a 35-mm glass bottom
29
30 dish with 4 chambers, a 20 mm microwell, and a #1 cover glass (0.13-0.16 mm). The amount of
31
32 the fluorescently labeled polymer-PIR conjugate added to the cell suspensions was normalized to
33
34 the DY-676 content (1 µg DY-676/mL), corresponding to the final conjugate concentration of
35
36 100 µg/mL. After 2, 4, 8, 16, 24 and 48 h, the native cells were washed three times with PBS and
37
38 the nuclei were with 5 µg/mL of Hoechst 33342. DY-676-labeled polymer conjugates were
39
40 excited at 674 nm and the emitted light was detected at 699 nm. PIR was excited at 488 nm and
41
42 the emission was measured through a 500 – 600 nm filter. Hoechst 33342 dye was excited at 405
43
44 nm and the emitted light was measured through a 450 – 500 nm filter. The fluorescence and
45
46 transmitted light was acquired using a laser scanning confocal microscope (LSCM) Olympus
47
48 IX83 with the FV10-ASW software (Olympus, Czech Republic). The samples were scanned with
49
50 a 60 × oil immersion objective Plan ApoN (1.42 numerical aperture; Olympus, Czech Republic).
51
52
53
54
55

56 *Competitive Hoechst staining - detection of doxorubicin in cell nuclei*

1
2
3 DLD-1 cells were incubated with free PIR or with the polymer-PIR conjugates at
4
5 concentration 100 – 0.01 $\mu\text{g}/\text{mL}$ of PIR under standard culture conditions. After 24 h, the cells
6
7 were detached with a detaching solution (100 mM HEPES, 20 mM NaCl, 10 mM EDTA, 0,5 %
8
9 BSA), stained with Hoechst 33342 (10 $\mu\text{g}/\text{mL}$) at 37 °C for 30 min and washed with ice-cold
10
11 PBS with BSA (0.5 %). The cells were immediately analyzed using a BD FACSVerse flow
12
13 cytometer (BD Biosciences, USA). The excitation wavelength for PIR was 488 nm and the
14
15 emission was measured through a 586BP42 pass filter; the Hoechst 33342 was excited at 405 nm
16
17 and the emission was detected through a 448BP45 filter. The data were analyzed in two
18
19 independent experiments. The medians of the fluorescence intensities were calculated using
20
21 FlowJo software (Tree Star, USA).
22
23
24
25
26
27

28 *Synthesis of monomers*

29
30 *N*-(2-Hydroxypropyl)methacrylamide (HPMA) was synthesized by reacting methacryloyl
31
32 chloride with (*RS*)-1-aminopropan-2-ol in dichloromethane in the presence of sodium carbonate
33
34 as described²⁸.
35
36

37 *N*-(*tert*-butoxycarbonyl)-*N'*-(6-methacrylamidohexanoyl)hydrazine (Ma-Ahx-NHNH-Boc)
38
39 was prepared in two-step process by the reaction of methacryloyl chloride with 6-aminohexanoic
40
41 acid in the presence of NaOH followed by the condensation of formed 6-
42
43 (methacryloylamino)hexanoic acid with *tert*-butyl carbazate in the presence of DCC²⁹.
44
45
46

47 *N*-Methacryloylglycylphenylalanylleucylglycine (MA-GFLG-OH) was prepared by automated
48
49 solid phase peptide synthesis on 2-chlorotrityl chloride resin starting from the C-terminus using
50
51 standard Fmoc procedures. 3-(*N*-Methacryloylglycylphenylalanylleucylglycine)thiazolidine-2-
52
53 thione (Ma-GFLG-TT) was prepared by reacting Ma-GFLG-OH with 4,5-dihydrothiazole-2-thiol
54
55 in DMF in the presence of DCC according to³⁰.
56
57
58
59
60

Synthesis of di-block copolymer precursors **PP2** – **PP4**

The thermo-responsive micelle-forming polymer precursors were produced as A-B type di-block copolymers by RAFT polymerization in two synthetic steps. The hydrophilic block A was prepared by copolymerizing HPMA with Ma-Ahx-NHNH-Boc using CPB as a chain transfer agent and AIBN as an initiator. The hydrophilic block A was subsequently subjected to a chain-extension polymerization through the RAFT mechanism with DEGMA to introduce the thermo-responsive polymer block B. Three different ratios of poly[(HPMA)-*co*-(Ma-Ahx-NHNH-Boc)], as the macro-chain transfer agent, to DEGMA were used to synthesize the di-block polymers with variable lengths of the thermo-responsive blocks.

Example: A mixture of 5.8 mg CPB (26.1 μmol) and 2.1 mg AIBN (13.0 μmol) was dissolved in 0.368 mL of DMSO and added to a solution of 500.0 mg HPMA (3.49 mmol) and 57.6 mg Ma-Ahx-NHNH-Boc (0.18 mmol) in 3.312 mL of *tert*-butanol. The reaction mixture was thoroughly bubbled with Ar and polymerized in the sealed glass ampoules at 70 °C for 6 h. The resulting copolymer was isolated by precipitation into a 3:1 mixture of acetone and diethyl ether and purified by gel filtration using a SephadexTM LH-20 cartridge in methanol. The methanolic solution was concentrated under reduced pressure and precipitated in diethyl ether yielding 268.3 mg (48.1 %) of the poly[(HPMA)-*co*-(Ma-Ahx-NHNH-Boc)] polymer precursor (PP1) as a pink powder. The content of dithiobenzoate (DTB) end groups was $n\text{DTB} = 60.3 \mu\text{mol/g}$, corresponding to $M_{n,\text{UV}} = 16,580 \text{ g/mol}$ ($f = 0.85$). Next, a solution of 50.0 mg **PP1** (3.01 μmol DTB groups) in 64.8 μL of deionized H₂O was added to a mixture of 21.6 mg DEGMA (0.12 mmol) and 0.1 mg AIBN (0.60 μmol) in 130 μL of 1,4-dioxane, thoroughly bubbled with Ar and allowed to polymerize in the sealed glass ampoules at 70 °C for 18 h. The di-block polymer was isolated by precipitation to diethyl ether yielding 63.8 mg (89.1 %) of the pale pink amorphous

1
2
3 solid. The precipitated polymer was dissolved in 638 μL of DMSO, 16.0 mg of ABIN (97.4
4
5 μmol) was added and the solution was heated up to 80 $^{\circ}\text{C}$ for 2 more hours. The resulting di-
6
7
8 block copolymer was isolated by precipitation in diethyl ether and purified by gel filtration using
9
10 the SephadexTM LH-20 cartridge in methanol. The methanolic solution was concentrated under
11
12 vacuum and precipitated in diethyl ether yielding 52.1 mg of the poly[(HPMA)-*co*-(Ma-Ahx-
13
14 NHNH-Boc)]-*block*-p(DEGMA) polymer as a white amorphous solid. The di-block copolymer
15
16 with Boc-protected hydrazide groups was suspended in 700 μL of TFA/TIPS/ H₂O (92 : 2.5 :
17
18 2.5) mixture and sonicated until all solids were dissolved (~5 min). Thereafter, the polymer was
19
20 precipitated into diethyl ether and re-dissolved in phosphate buffer (0.15 M, pH 8.0). The pH of
21
22 the solution was adjusted to 7.4 using a NaOH solution and the polymer was desalted by the
23
24 SephadexTM PD-10 column in H₂O. The resulting polymer precursor poly[(HPMA)-*co*-(Ma-
25
26 Ahx-NHNH₂)]-*block*-p(DEGMA) (**PP2**) was isolated from an aqueous solution by lyophilization
27
28 yielding 48.3 mg of the white solid. The reaction conditions for all synthesized polymer
29
30 precursors (**PP1** – **PP4**) as well as their physicochemical characteristics are summarized in the
31
32 Table 1.
33
34
35
36
37
38
39

40 *Synthesis of hydrophilic copolymer precursor PP6*

41
42 The copolymer precursor poly[(HPMA)-*co*-(Ma-GFLG-TT)] (**PP6**) was prepared by RAFT
43
44 polymerization of 200.0 mg HPMA (1.40 mmol) and 87.0 mg Ma-GFLG-TT (0.15 mmol) using
45
46 0.64 mg AIBN (3.90 μmol) as an initiator and 1.72 mg CTP (6.16 μmol) as a chain transfer
47
48 agent. The polymerization mixture was dissolved in 1.563 mL of *tert*-butanol with 10 % DMSO,
49
50 transferred into a glass ampoule, bubbled with Ar and sealed. After 24 h at 70 $^{\circ}\text{C}$, the product
51
52 was isolated by precipitation of the reaction mixture to acetone/diethyl ether (3:1); the precipitate
53
54 was then washed with diethyl ether and dried under vacuum. This product was then reacted with
55
56
57
58
59
60

1
2
3 AIBN (10 molar excess) in DMSO (15% w/w solution of polymer) under Ar for 3 h at 70 °C in a
4 sealed ampoule to remove DTB end groups. The reaction mixture was isolated by precipitation
5 in acetone/diethyl ether (3:1); the precipitate was washed with diethyl ether and dried under
6 vacuum to yield 186.5 mg of copolymer precursor **PP6**. The number-average molecular weight
7 (M_n) of the copolymer was 35,500 g/mol and polydispersity index (D) was 1.12. The content of
8 TT groups (φ^{TT}) was 6.8 mol. %.

17
18
19 *Attachment of PIR and fluorophore to the di-block copolymer precursors (PC2F – PC4F)*

20
21 Pirarubicin was attached to the hydrazide groups distributed along the hydrophilic block A of
22 the copolymer precursors through the hydrolytically degradable hydrazone bond. For the FACS
23 analysis (see above), some of the hydrazide groups of the copolymers were used for the
24 copolymer labeling with a fluorescent dye via the stable diacylhydrazine bonds.

25
26 Example: A mixture of 20.0 mg **PP2** and 0.4 mg DY-676 NHS-ester (0.44 μmol) was
27 dissolved in 80 μL of DMA and the solution was stirred for 4 h at r.t. Then, 2.2 mg PIR (3.5
28 μmol) in 80 μL of methanol and 8 μL of acetic acid was added drop-wise and the reaction
29 mixture was stirred for another 18 h at r.t. The resulting polymer conjugate (**PC2-F**) was
30 separated from the reaction mixture by gel filtration using the SephadexTM LH-20 column in
31 methanol followed by inspissation of the methanolic solution on a rotary evaporator and
32 precipitation of the conjugate in ethyl acetate yielding 12.6 mg of the dark violet solid. The
33 physicochemical characteristics for the polymer-PIR conjugates are summarized in Table 2.

34
35
36
37
38
39
40
41
42
43
44
45
46
47
48
49
50 *Attachment of PIR to the hydrophilic copolymer precursor (PC6)*

51
52 A mixture of 92.0 mg **PP6** (36.5 μmol TT) and 7.9 mg PIR (12.6 μmol) was dissolved in 1.75
53 mL of DMA and stirred at r.t. The yield of the reaction was monitored by HPLC. After 3 h, when
54 the reaction was completed, 4.3 μL of (*RS*)-1-aminopropan-2-ol (54.8 μmol) was added to the
55
56
57
58
59
60

1
2
3 reaction mixture to quench the unreacted TT. After another 30 min, the polymer conjugate was
4
5 isolated by precipitation of the reaction mixture in ethyl acetate and the precipitate was
6
7 centrifuged. The precipitate was washed with diethyl ether and dried under vacuum yielding 84.0
8
9 mg of **PC6**. $M_n = 41,000$ g/mol, $D = 1.17$ and $\omega^{\text{PIR}} = 9.0$ wt. %. The chemical structure of **PC6**
10
11 conjugate is shown in Figure S1 B.
12
13
14
15

16 **Results and discussion**

17 *Polymer-PIR conjugates synthesis*

18
19
20 The synthesis of the polymer-PIR conjugates was carried out in two synthetic steps, including
21
22 the synthesis of the amphiphilic di-block copolymer precursors, followed by the attachment of
23
24 either the cancerostatic drug pirarubicin or the fluorescent dye. The precursors (**PP1 – PP4**) were
25
26 synthesized by the RAFT polymerization technique, enabling the synthesis of highly defined
27
28 uniform materials with predetermined molecular weights and high yield of DTB end-group
29
30 content. The hydrophilic block (PP1) was prepared by copolymerizing HPMA with Ma-Ahx-
31
32 NHNH-Boc using the DTB-derived chain transfer agent (see Scheme 1). The copolymer with M_n
33
34 = 14,100 g/mol was distinguished by narrow molecular weight distribution ($M_w/M_n = 1.11$) and
35
36 sufficient functionality ($f = 0.85$) of the DTB end groups. The functionality of the polymer (f , the
37
38 amount of the functional end groups per one polymer chain) was defined as the ratio between M_n
39
40 obtained from the SEC measurement and $M_{n,UV}$ calculated from the end group analysis. The
41
42 content of comonomer units bearing the hydrazide groups, determined by TNBSA assay (after
43
44 removal of Boc protective groups, see Experimental section) and confirmed by $^1\text{H-NMR}$
45
46 spectroscopy (data not shown) was 4.8 mol. %, which is equal (within experimental error) to the
47
48 quantity of Ma-Ahx-NHNH-Boc (5.0 mol. %) in the polymerization feed. The precursor **PP1**
49
50 was further used as the macro-chain transfer agent for the subsequent chain extension with the
51
52
53
54
55
56
57
58
59
60

1
2
3 thermo-responsive poly(DEGMA) blocks. Three different ratios of DEGMA to DTB-end groups
4 of **PP1** were used (see Table 1) to synthesize the amphiphilic di-block copolymers with variable
5 lengths of the thermo-responsive block ranging from approximately 7,000 to 24,600 g/mol. The
6 incorporation of poly(DEGMA) blocks to the HPMA-based copolymer precursor resulted in a
7 moderate broadening of the distribution of molecular weights ($M_w/M_n \approx 1.5$). This can be
8 ascribed to a low but not insignificant quantity of **PP1** dead chains (not terminated with DTB
9 groups) that could not react further with DEGMA through the RAFT mechanism. Consequently,
10 the resulting precursors were the mixture of two polymer populations with different molecular
11 weights – the largely prevailing di-block copolymer and a small amount of initial hydrophilic
12 precursor (Figure 1).
13
14
15
16
17
18
19
20
21
22
23
24
25
26

27 To prevent the unwanted reactions of DTB end groups of the polymers with the hydrazide side
28 chain groups during the removal of Boc protective groups or with PIR during the following
29 conjugation, the DTB groups were removed by a reaction with a high molar excess of AIBN
30 through the homolytic mechanism. The replacement of DTB groups by the isobutyronitrile
31 groups was documented by the disappearance of the UV absorption peak at 302 nm. Finally, Boc
32 groups protecting the hydrazides were quantitatively removed using the TFA/TIPS/H₂O mixture,
33 commonly used in peptide chemistry, yielding the polymer precursors **PP2** – **PP4**. Neither the
34 DTB group substitution nor the removal of Boc groups caused significant changes in the
35 molecular weights and molecular weight distributions of the polymer precursors. The molecular
36 weight parameters for **PP2** – **PP4** are summarized in Table 1 and SEC profiles are depicted in
37 Figure 1.
38
39
40
41
42
43
44
45
46
47
48
49
50
51
52

53 The conjugation of PIR to the copolymer precursors was achieved by the hydrazone bonds
54 formed between the keto group of PIR and the hydrazide groups in the side chains of polymers
55
56
57
58
59
60

1
2
3 (the reaction scheme is shown in Scheme 2, an example of SEC chromatogram for the conjugate
4
5 **PC2** recorded by LS, RI and UV detectors is depicted in Figure S2 B). Based on our previous
6
7 experiences with the structurally similar cancerostatic drug doxorubicin (DOX), the reaction was
8
9 performed in methanol in the presence of acetic acid³¹. The yields of the conjugation reaction
10
11 ranged between 70 and 80 %. The method of PIR attachment was selected with respect to the
12
13 pH-controlled stability of the hydrazone bond – relatively stable at neutral pH but susceptible to
14
15 much faster hydrolysis in mildly acidic conditions. This approach is very beneficial for a
16
17 systemic administration because the majority of the drug remains attached to the polymer carrier
18
19 during its transport in the bloodstream (pH 7.4) but is released in the target tumor cells (pH 5.5).
20
21 To verify this claim, we measured the release of PIR from conjugates **PC2 – PC4** under
22
23 physiological environment-modeling conditions (see Experimental section) at both relevant pH
24
25 values. As shown in Figure 2A, the rate of the hydrazone bond hydrolysis proceeded much faster
26
27 in solutions with a lower pH, which documents the suitability of the conjugates for safe drug
28
29 delivery purposes. Although the ability of the conjugates to release PIR under the conditions
30
31 modeling the intratumoral environment is evident, it appears that the conjugates in aqueous
32
33 solution still contain approximately 35 – 40 % of bound PIR even after 24 h of acidic hydrolysis
34
35 at pH 5.5. This can be explained by the hydrophobic character of the poly(DEGMA) chains
36
37 retaining the already released hydrophobic drug packed inside the polymer coil by hydrophobic
38
39 interactions upon disruption of the hydrazone bond. The hydrophobic retention of PIR by the
40
41 polymer coil increased with increasing poly(DEGMA) block length. The release of PIR was also
42
43 evaluated by GPC analysis with the methanol/sodium acetate buffer (80:20) mixture as a mobile
44
45 phase (see Experimental section). In the methanolic solution, the hydrophobic interaction
46
47
48
49
50
51
52
53
54
55
56
57
58
59
60

1
2
3 between the polymer and the released drug was disrupted, which resulted in an almost complete
4 release of PIR from the carrier by hydrolysis (see Figure 2B).
5
6

7
8 For the laser scanning confocal microscopy (LSCM) measurement of the interaction of the
9 conjugates with the cells, the polymer precursors **PP2 – PP4** were modified (in a one-pot
10 reaction together with PIR) with DY-676 NHS ester fluorescent dye (**PC2F – PC4F**) that emits
11 light in a different region of the light spectrum than PIR (see Experimental section). Because the
12 fluorescent dye was attached to the polymer backbone of the conjugates through the stable
13 diacylhydrazine bonds (see Scheme 2), the LSCM images enabled a simultaneous observation of
14 the intracellular fate of the polymer and PIR (both bound and released) over time. However, we
15 would like to note that the apparent molecular weights of the fluorescently labeled polymer-PIR
16 conjugates, measured by GPC equipped with a LS detector, were approximately 1.5 times higher
17 than those of the corresponding polymer precursors. Because no broadening of the molecular
18 weight distributions was observed, we hypothesize that this difference was due to the
19 contribution of PIR fluorescence to the intensity of the light scattering. Therefore, it was
20 necessary to calculate the molecular weights by a "relative" molecular weight determination
21 method using a series of well-characterized poly(HPMA) polymer standards. The molecular
22 weights of such characterized conjugates were only approximately 3 - 5 % higher than those of
23 the corresponding precursors, which is in good agreement with the theoretical expectation.
24 Complete physicochemical characteristics of the polymer-PIR conjugates, including the
25 corrected MWs are summarized in **Error! Reference source not found.**
26
27
28
29
30
31
32
33
34
35
36
37
38
39
40
41
42
43
44
45
46
47
48
49
50

51 *Solution behavior of thermo-responsive polymer-PIR conjugates*

52
53
54 The temperature-dependent changes in solution behavior of the polymer-PIR conjugates and
55 their corresponding precursors were studied by DLS. We focused on the influence of the
56
57
58
59
60

1
2
3 composition and structural parameters of the polymers on their hydrodynamic properties in the
4 solutions mimicking physiological conditions as our understanding of such properties may play
5 an important role in the design of drug delivery systems for efficient *in vivo* treatment. First, we
6 clearly demonstrated that the hydrophobic poly(DEGMA) block length (MW) is the decisive
7 structural factor. Specifically, an increase in molecular weight of the poly(DEGMA) block (at a
8 constant MW of the hydrophilic block) caused not only a decrease in transition temperatures (T_{tr})
9 of the copolymers but also resulted in the formation of larger-sized polymer coils (below T_{tr}) and
10 larger-sized polymer micelles (above T_{tr}) (see Figure 3). For example, the **PP2** precursor with
11 MW of the hydrophilic block almost two-times higher than the hydrophobic block showed a T_{tr}
12 18 °C higher than poly(DEGMA) homopolymer ($T_{tr} \approx 26$ °C), while in the case of **PP4**, where
13 the MW of the hydrophobic block is 1.7 times higher than MW of the hydrophilic block, the T_{tr}
14 of the copolymer is only slightly higher in comparison to poly(DEGMA) itself. Based on these
15 observations (and also our understanding of the dependence of T_{tr} on MW of other thermo-
16 responsive polymers) it is reasonable to predict that further poly(DEGMA) chain lengthening
17 would not result in significant T_{tr} decrease. Additionally, an increase in the polymer micelle sizes
18 of the **PC2 – PC4** conjugates with increasing MW of poly(DEGMA) chains was predictable
19 because longer polymer chains self-assembled into larger-sized nanoparticles. The length of the
20 hydrophobic block has also an impact on the micelle stabilities expressed by the critical micellar
21 concentration (CMC) values. It was shown that the CMC values decreased (stabilities of the
22 conjugates increased) with increasing MW of the poly(DEGMA) blocks from 0.071 mg/mL for
23 **PC2** up to 0.022 mg/mL for **PC4**. Considering the usual concentrations (~10 mg PIR/kg of
24 mouse body weight, *i.v.* injection) of the previously described polymer-PIR conjugates in mice
25 experiments³², the CMC values acquired for **PC2 – PC4** guarantee, with a sufficient reserve,
26
27
28
29
30
31
32
33
34
35
36
37
38
39
40
41
42
43
44
45
46
47
48
49
50
51
52
53
54
55
56
57
58
59
60

1
2
3 that the thermo-responsive conjugates will exist in their micellar form even after their injection
4
5 to the mice. This interesting finding brought a comparison of T_{tr} of the polymer precursors and
6
7 the polymer-PIR conjugates. As shown in Figure 3, the incorporation of the hydrophobic drug to
8
9 the polymers caused a marked decrease in T_{tr} (by ~ 5 °C) regardless of the poly(DEGMA) block
10
11 length. Because PIR is attached to the polymers through hydrolytically degradable bonds, it is
12
13 reasonable to expect that T_{tr} of the conjugates will increase upon PIR release inside the cells (an
14
15 example of increase of T_{tr} of the conjugate **PC2** after 24 h of hydrolysis carried out under model
16
17 conditions (PBS, pH 5.5, 37 °C) is shown in Figure S3). This increase in T_{tr} can be employed in
18
19 the design of biodegradable micelle-based drug delivery systems. Such drug-bearing conjugates
20
21 can reach the target tumor cells in their micellar form ($T_{tr} < 37$ °C) through the EPR effect, but
22
23 the drug-free copolymer ($T_{tr} > 37$ °C) can be reliably eliminated from the body as an unimer
24
25 (single copolymer molecules) formed upon PIR release, through renal filtration. From this point
26
27 of view, the conjugate **PC3** exhibited the most favorable properties. It formed a polymer micelle
28
29 spontaneously under physiological conditions, but began to change its morphology to random
30
31 coil during PIR cleavage from the polymer. As shown at Figure 4, polymer conjugate **PP3** (the
32
33 precursor of **PC3**) at 37 °C is predominantly in the micellar form, however, a significant portion
34
35 of the polymer is present already in the form of unimers. To the contrary, the conjugate **PC2**
36
37 adopted the random coil formation both before and after PIR release and the conjugate **PC4**
38
39 existed only as a fully solvated unimer regardless of attached or released PIR (see Figure 3 and
40
41 4).
42
43
44
45
46
47
48
49

50 51 52 *Cytotoxicities of the polymer-PIR conjugates*

53
54 The cytotoxicities of PIR and the polymer-PIR conjugates were reported as IC_{50} values, which
55
56 is the concentration of material at which 50 % of the cell culture is no longer viable. In this
57
58
59
60

1
2
3 experiment, we used the human colorectal adenocarcinoma (DLD-1) and the mouse lymphoma
4 (EL-4) cell lines, both relevant models to this study. According to the results in Table 3, the IC₅₀
5 values of the thermo-responsive polymer-PIR conjugates **PC2 – PC4** are all very similar
6 (approximately 3 µg/mL against DLD-1 cell line and 0.01 µg/mL against EL-4 cell line).
7
8 However, these values are approximately 20 times higher (in the case of DLD-1 cells) than those
9 for free PIR. This finding demonstrates that the attachment of the drug to the polymer carriers
10 significantly reduces its direct cytotoxicity and, at the same time, that the poly(DEGMA) block
11 length nowise affects the toxicity of the conjugates. Lower conjugate toxicity is favorable
12 because it enables the administration of the drug at a higher concentration, thus increasing the
13 potential therapeutic effect. The comparison of the thermo-responsive polymer-PIR conjugates
14 **PC2 – PC4** with the linear hydrophilic polymer-PIR conjugates containing the drug attached to
15 the polymer backbone either through the hydrolytically degradable hydrazone bond (**PC5**) or
16 through the enzymatically degradable tetrapeptide spacer GFLG (**PC6**) led to interesting results.
17 While the cytotoxicity of the conjugate **PC5** was approximately 2 times (for the DLD-1 cells), or
18 100 times (for the EL-4 cells) higher than that for **PC2 – PC4** (not statistically significant
19 differences), the conjugate **PC6** was approximately 5 times less toxic (for DLD-1 cells) than the
20 thermo-responsive ones (statistically significant differences). The higher toxicity of the **PC5**
21 conjugate can be ascribed to the more hydrophilic character of its polymer backbone enabling
22 faster release of PIR from the carrier without its subsequent retention due to hydrophobic
23 interaction with the hydrophobic block of the copolymer (see ref. ³³). To the contrary, conjugate
24 **PC6**, although having PIR bound via the enzymatically degradable GFLG linker, released only a
25 modest amount of the drug within the monitored time interval. This is in agreement with a
26 published observation ^{34,35}. The polymer precursors **PP2 – PP4** showed no toxicity. The
27
28
29
30
31
32
33
34
35
36
37
38
39
40
41
42
43
44
45
46
47
48
49
50
51
52
53
54
55
56
57
58
59
60

1
2
3 pronounced differences of approximately two orders of magnitude in the IC₅₀ values measured in
4
5 DLD-1 and EL-4 cells are caused by the different sensitivity of the two cell lines to PIR.
6
7

8 9 *Internalization of the polymer-PIR conjugates into cells*

10
11 The intracellular fate of the polymer-PIR conjugates and free PIR was observed in DLD-1
12 cells by LSCM at different time points (see Experimental Section). The fluorescent signal of the
13
14 DY-676-labeled polymer conjugates increased over time for all studied samples. As shown in
15
16 Figure 5, there are obvious differences in the intracellular localization and the mechanism of
17
18 action between free PIR, the thermo-responsive polymer-PIR conjugates and the control
19
20 hydrophilic polymer-PIR conjugates. While in the case of free PIR and the control polymer-PIR
21
22 conjugate having PIR attached through the hydrolytically degradable bond (**PC5**) a substantial
23
24 amount of the drug was detected in the cytoplasm and inside the cell nuclei, in the case of the
25
26 thermo-responsive polymer-PIR conjugates (**PC2 – PC4**) and the control hydrophilic polymer-
27
28 PIR conjugate having PIR attached through the enzymatically degradable GFLG spacer (**PC6**)
29
30 PIR was predominantly detected in the cytoplasm and on the surface of the nuclear membrane.
31
32 The fact that only a very small amount of PIR was found in the cell nuclei can be probably
33
34 attributed to the hydrophobic retention of the released PIR in the hydrophobic poly(DEGMA)
35
36 domains of copolymers **PC2 – PC4** and the relatively slow enzymatic cleavage of the GFLG
37
38 tetrapeptide spacer in copolymer **PC6** by lysosomal proteases^{34, 35}. Surprisingly, although the
39
40 structure and chemical composition of the two types of conjugates (**PC2 – PC4** and **PC6**) is
41
42 different, their intracellular fate, according to the LSCM study, seems to be quite similar. These
43
44 polymer/PIR conjugates probably interact hydrophobically with the lipid bilayer of the cell
45
46 nucleus, thereby decreasing the membrane permeability and preventing further progression of the
47
48 cells. LSCM showed that the cells incubated with the **PC2 – PC4** and **PC6** conjugates
49
50
51
52
53
54
55
56
57
58
59
60

1
2
3 significantly changed their morphology and size of the intracellular compartments, namely the
4 nuclei, in comparison with the non-treated cells (not shown) and the cells treated with PIR or
5 **PC5** conjugate. This behavior of the cells resembles the phenomenon called oncosis, a non-
6 apoptotic mode of cell death, characterized by mitochondrial swelling, cytoplasm vacuolization,
7 and swelling of the nucleus and cytoplasm³⁷. Moreover, the cells treated with **PC2 – PC4** and
8 **PC6** conjugates showed reduced amount of the mutual intracellular connections documenting an
9 apparent damage of the cells. Because the polymer precursors **PP2 – PP4** without PIR were non-
10 toxic and did not affect the morphology of the cancer cells (LSCM images not shown), it is
11 obvious that the polymer carriers alone were not responsible for the observed cytotoxic effect of
12 the conjugates. In this experimental setting, no pronounced difference in the behavior of cells
13 treated with individual thermo-responsive polymer-PIR conjugates **PC2 – PC4** and polymer
14 **PC6** on the cancer cells was observed. It appears that the poly(DEGMA) block, regardless of its
15 length, is the principal structural factor of the polymer-PIR conjugates influencing their
16 biological behavior. As already mentioned, despite the significant structural differences between
17 the thermo-responsive polymer-PIR conjugates **PC2 – PC4** and hydrophilic polymer-PIR
18 conjugate **PC6**, the LSCM images documenting the intracellular fate of the conjugates are
19 strikingly similar. We can hypothesize that both types of conjugates exhibit an amphiphilic
20 character (due to the presence of thermo-responsive poly(DEGMA) block in conjugates **PC2 –**
21 **PC4** and a hydrophobic GFLG spacer between PIR and polymer backbone in conjugate **PC6**)
22 that might be responsible for the non-specific interaction of the polymer conjugates with various
23 membrane structures inside the cells. The detailed analysis of the intracellular behavior of the
24 conjugates and the mechanism of their action in the cancer cells will be the subject of our
25 upcoming publication.

Incorporation of PIR into the cell nuclei

To verify the results from LSCM images, the Hoechst incorporation assay using FACS analysis was performed. The cells (DLD-1) were incubated with a concentration array of the polymer-PIR conjugates or free PIR for 24 h followed by the addition of Hoechst 33342, an intercalating fluorescent dye used for DNA staining. The assay is based on the characteristics of PIR to intercalate between the base pairs of DNA strands and thus block the subsequent interaction of DNA with Hoechst. In other words, the Hoechst dye can insert only in sections of DNA strands that are not occupied by PIR. The results of intercalating competitions between the DNA/PIR complexes and the Hoechst 333258 dye for the individual polymer-PIR conjugates as well as for free PIR are shown in Figure 6. The highest intercalation ability showed free PIR whose concentration in the cell nuclei gradually increased (the concentration of Hoechst in the cell nuclei gradually decreased) from 1 $\mu\text{g/mL}$ to 100 $\mu\text{g/mL}$, at which point almost all intercalating sites of DNA were occupied by PIR (no Hoechst was detected). A slightly lower intercalation efficiency was found in the case of **PC5** conjugate where a sharp increase in PIR fluorescence intensity was observed starting from 10 $\mu\text{g/mL}$ of PIR. However, as in the previous case, DNA was fully saturated with PIR at a concentration of 100 $\mu\text{g/mL}$. This demonstrates the successful hydrolysis of the hydrazone bond, release of PIR from the conjugate and its subsequent penetration in the nucleus. Markedly different results were obtained when the cells were incubated with the **PC6** conjugate. Although PIR started incorporating slightly in the nuclei at a concentration 1 $\mu\text{g/mL}$, the efficiency of its intercalation was relatively low, which enabled the Hoechst dye to interact with DNA too. Only in the case of the highest concentration of the conjugate (100 $\mu\text{g/mL}$ of PIR), the amount of incorporated Hoechst decreased. This can be ascribed to a very low rate of PIR release from the conjugate due to the relatively slow gradual

1
2
3 enzymatic cleavage of the GFLG spacer between the drug and the polymer backbone^{34, 35} and
4
5 possibly also the hydrophobic retention of the released drug within the polymer coil containing
6
7 amphiphilic GFLG peptides. Similar results were also observed in cells incubated with the
8
9 thermo-responsive **PC2 – PC4** conjugates. In all cases, the Hoechst dye was incorporated in
10
11 DNA in the entire range of concentration of the conjugates (0.01 – 100 µg/mL of PIR),
12
13 indicating the low level of PIR intercalated in the cell nuclei even at the highest conjugate
14
15 concentration. These results are in good agreement with the LSCM pictures, in which almost no
16
17 PIR signal from the **PC2 – PC4** conjugates was detected inside the nuclei. This confirms our
18
19 hypothesis that PIR remains hydrophobically entrapped inside the coil of the thermo-responsive
20
21 polymers even after the hydrazone bond hydrolysis inside the cells. Furthermore, it seems that
22
23 this interaction is independent of the poly(DEGMA) block length, or more precisely, of the
24
25 conjugate morphology.
26
27
28
29
30
31

32 **Conclusion**

33
34
35
36 Conjugates of nano-sized polymer carriers with chemotherapeutics are considered to be a very
37
38 promising drug delivery system intended for the treatment of neoplastic diseases. The major
39
40 benefit is in their high ability for passive accumulation in solid tumors due to the EPR effect,
41
42 while causing minimal damage to healthy tissues. However, the clinical application of the
43
44 majority of the nanoparticle-based carriers encounters obstacles related to their relatively
45
46 laborious preparation, high tendency to aggregate, limited drug loading and complicated long-
47
48 term storage. Therefore, in this work, we focused on the development of novel thermo-
49
50 responsive polymer carriers characterized by relatively easy and reproducible preparation,
51
52 precisely defined chain structure with multiple binding sites for covalent attachment of drugs, an
53
54 adjustable unimer - micelle transition temperature and long-term stability. The di-block polymer
55
56
57
58
59
60

1
2
3 carriers, synthesized by RAFT polymerization, were comprised of a multivalent HPMA-based
4 hydrophilic block and a thermo-responsive DEGMA-based block of various lengths. The
5
6 cancerostatic drug pirarubicin (PIR) was conjugated to the hydrophilic blocks of the copolymers
7
8 via a hydrolytically cleavable hydrazone bond. The polymer-PIR conjugates showed
9
10 spontaneous pH-driven hydrolysis of the hydrazone bonds; PIR release proceeded much faster at
11
12 pH 5.5, corresponding to the intracellular environment than at pH 7.4, corresponding to the blood
13
14 circulation, thus meeting the requirements for safe delivery of the drug to cancer cells. The
15
16 conjugates underwent reversible temperature-induced conformation changes from random coils
17
18 to stable nano-sized micelles; the micelle size and stability as well as the transition temperature
19
20 of the conjugates were driven by the thermo-responsive block length and PIR content in the
21
22 range of 26 to 39 °C. All studied conjugates, regardless of thermo-responsive block length,
23
24 showed significantly lower cytotoxicity than free PIR (both in DLD-1 and EL-4 cells) and
25
26 demonstrated the ability to effectively penetrate the cell membrane of model cancer cell lines
27
28 (DLD-1). Although a considerable amount of PIR remained hydrophobically attached to the
29
30 polymer carrier even after the hydrazone bond disruption inside the cells, the resulting
31
32 polymer/PIR associates surrounded the cell nuclei membranes and blocked the transport through
33
34 the membrane. This led to changes in cell morphology and disrupted mutual intracellular
35
36 connections, indicating approaching cell death. Based on these encouraging results, we believe
37
38 that the studied conjugates have a great potential to become efficacious in vivo pharmaceuticals.
39
40
41
42
43
44
45
46
47
48
49
50
51
52
53
54
55
56
57
58
59
60

Figures

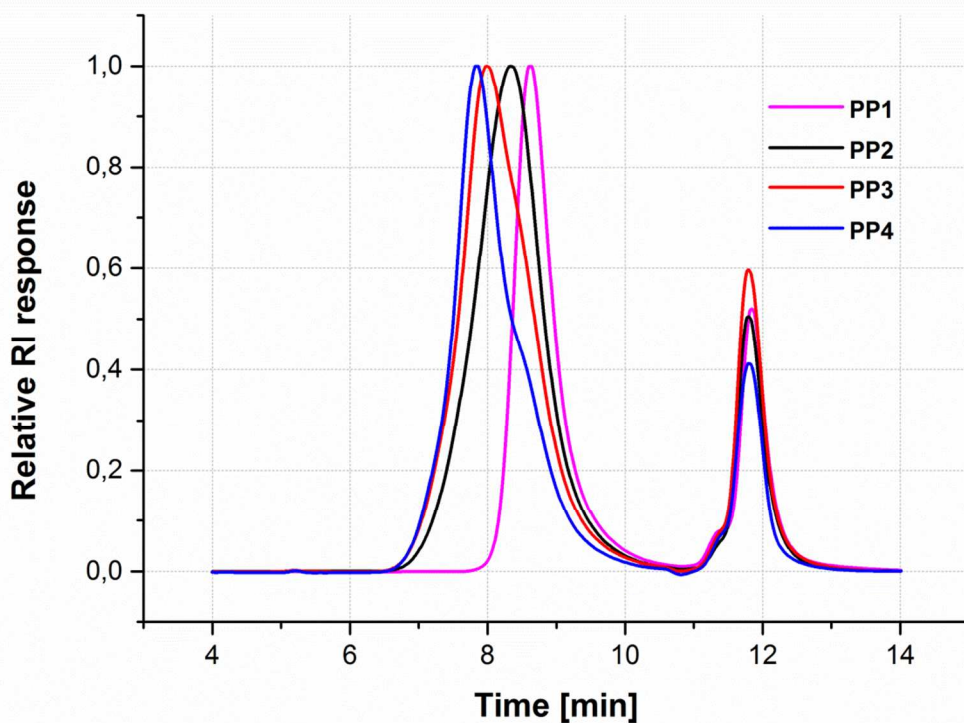
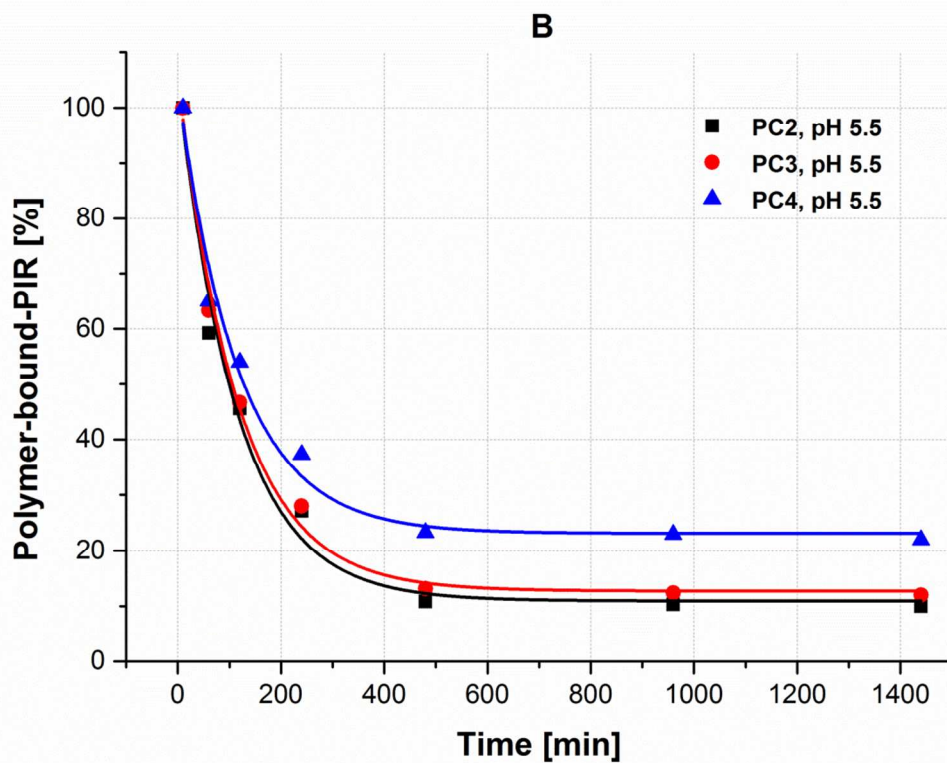
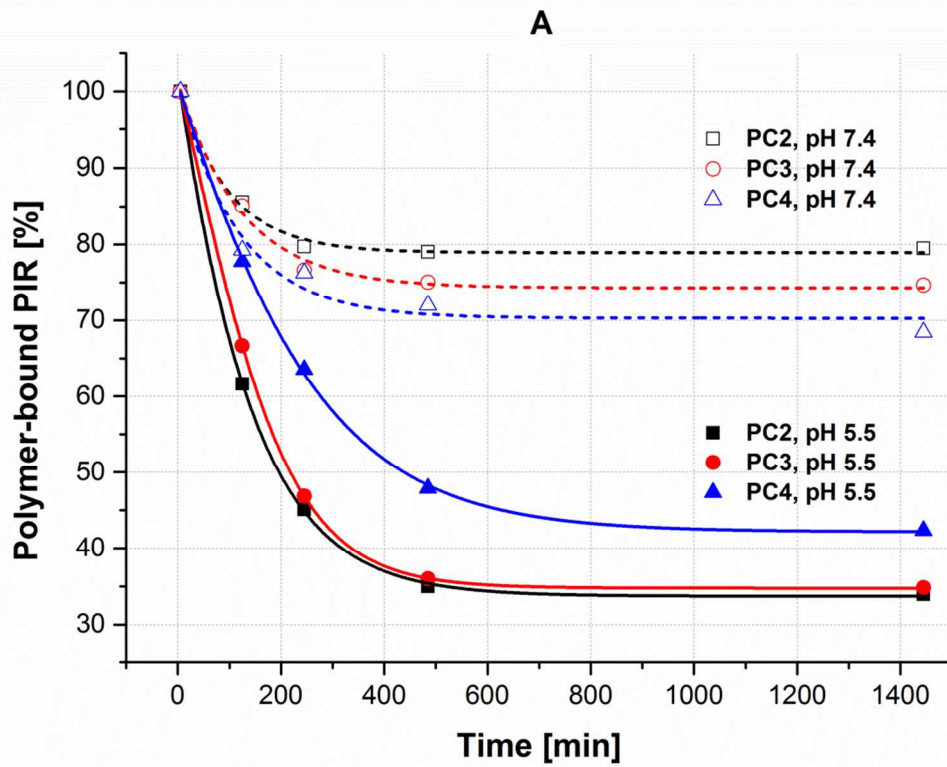
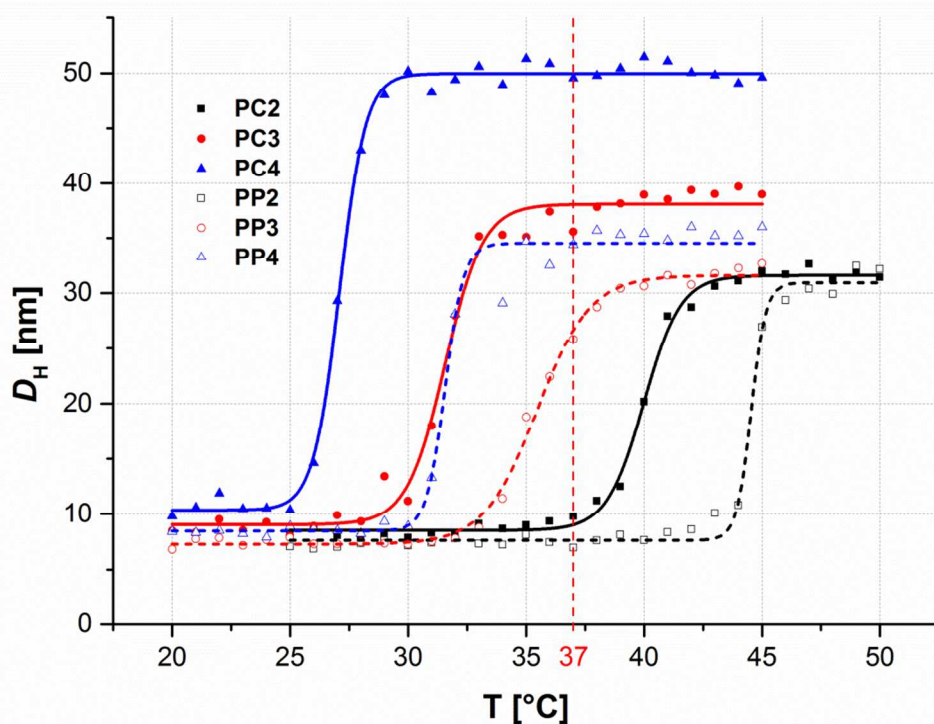


Figure 1. SEC profiles of the copolymer precursors **PP1 – PP4** plotted as a function of time of the normalized RI responses.



1
2
3
4 **Figure 2.** Release of PIR from the polymer-PIR conjugates **PC2 – PC4** incubated in phosphate
5 buffers at pH 7.4 (dashed lines) and pH 5.5 (solid lines) at 37 °C. Quantification of the polymer-
6 bound PIR was performed using the UV/VIS spectrophotometry by measuring the absorbance of
7
8 bound PIR was performed using the UV/VIS spectrophotometry by measuring the absorbance of
9
10 the polymer-PIR conjugates separated from free PIR by GPC carried out either in (A) PBS or in
11
12 (B) methanol/sodium acetate buffer (80:20) mixture.
13
14
15
16
17
18
19



20
21
22
23
24
25
26
27
28
29
30
31
32
33
34
35
36
37
38
39
40
41
42
43
44 **Figure 3.** Temperature dependence of the hydrodynamic diameters (D_H) of polymer-PIR
45 conjugates **PC2 - PC4** (solid lines) and their corresponding precursors **PP2 – PP4** (dashed lines)
46
47 measured by DLS.
48
49
50
51
52
53
54
55
56
57
58
59
60

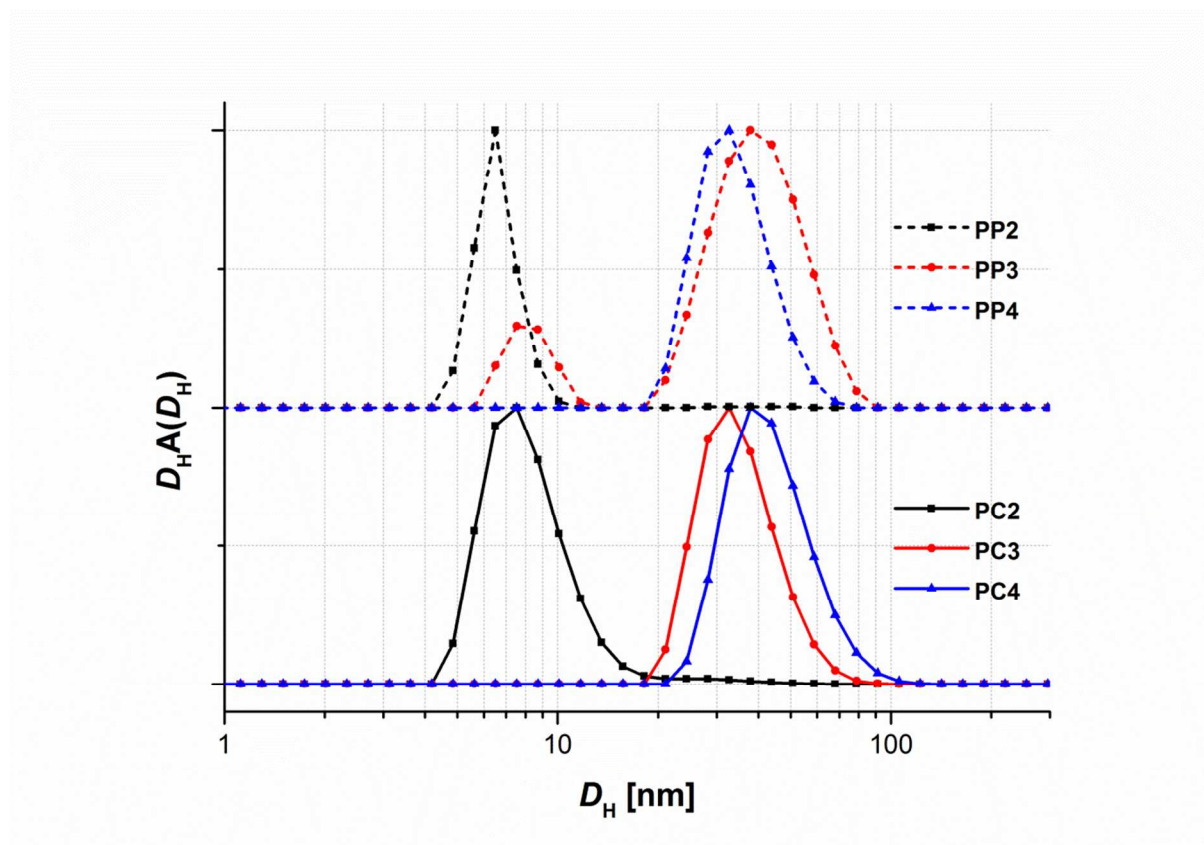
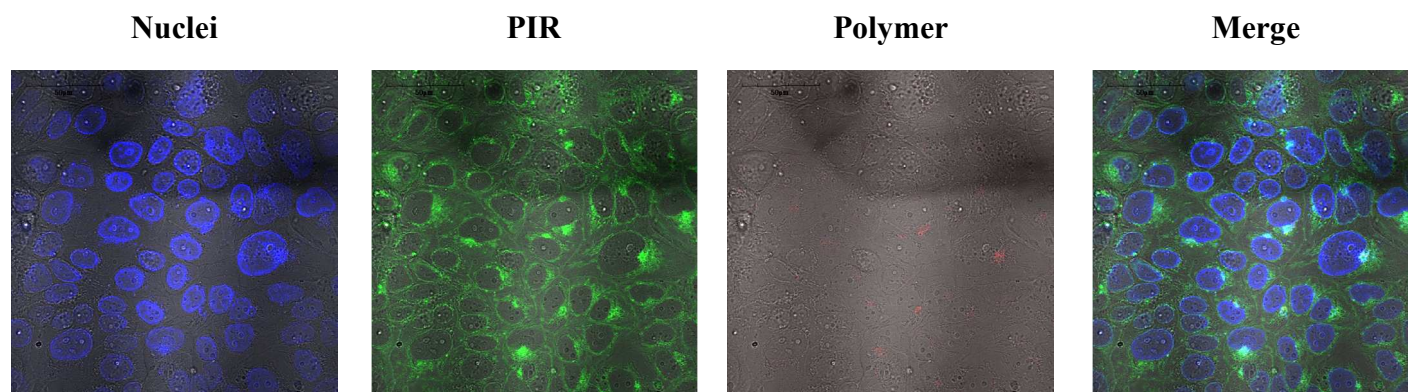
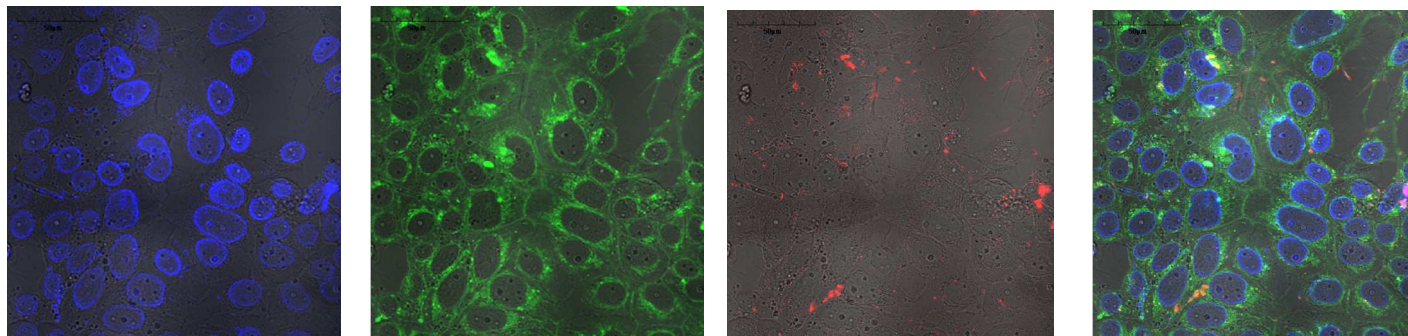


Figure 4. Normalized D_H -distribution function, $A(D_H)$, of polymer-PIR conjugates **PC2 – PC4** (solid lines) and their corresponding precursors **PP2 – PP4** (dashed lines) measured by DLS.

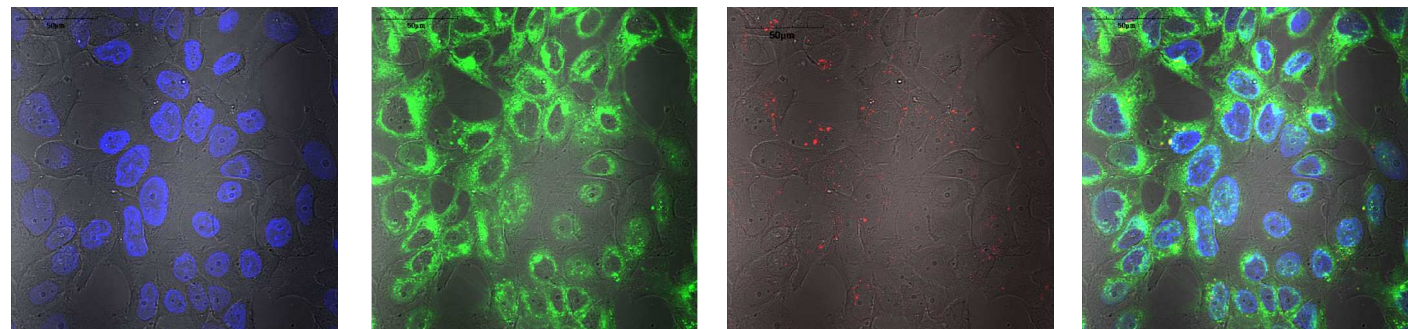


1
2
3
4
5
6
7
8
9
10
11
12
13
14
15
16
17
18
19
20
21
22
23
24
25
26
27
28
29
30
31
32
33
34
35
36
37
38
39
40
41
42
43
44
45
46
47
48
49
50
51
52
53
54
55
56
57
58
59
60

PC3



PC4

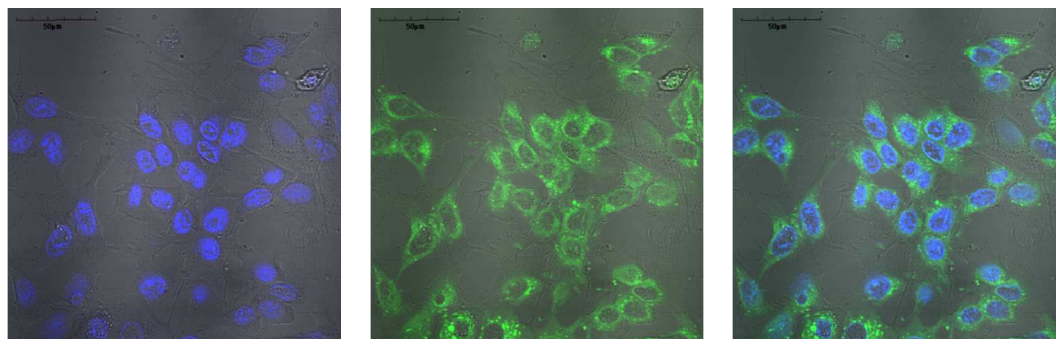


Nuclei

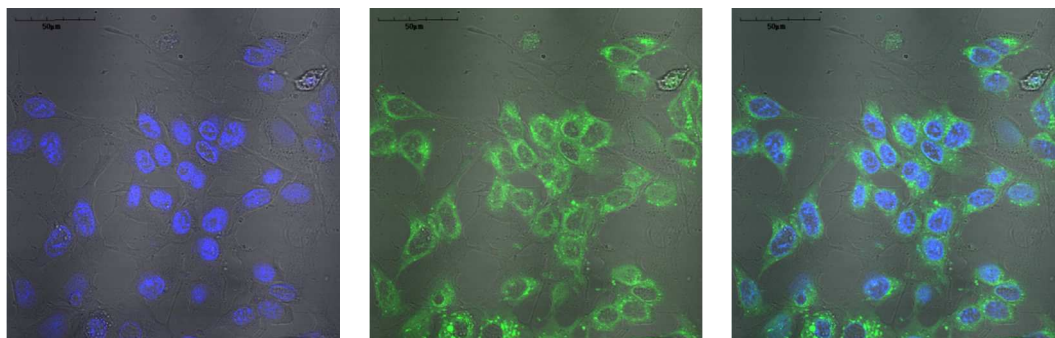
PIR

Merge

PIR



PC5



PC6

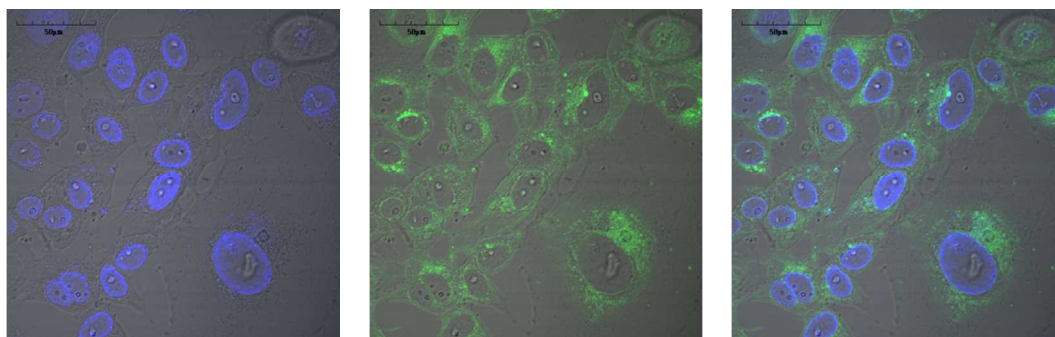
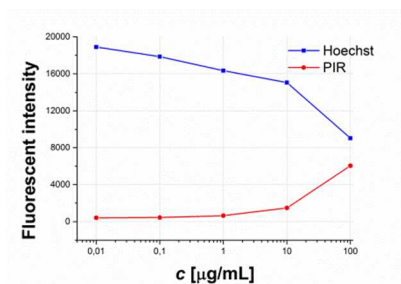
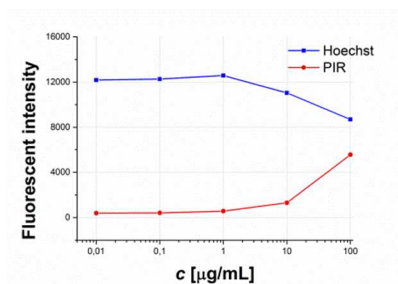


Figure 5. LSCM images of polymer-PIR conjugates and free PIR in DLD-1 cell lines after 24 h of incubation. Hoechst 333258 dye was used for the visualization of cell nuclei (blue color) and Dyomics-676 dye was used for the visualization of the polymers (red color). Green color represents PIR.

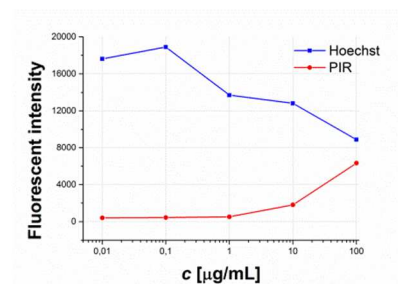
PC2



PC3



PC4



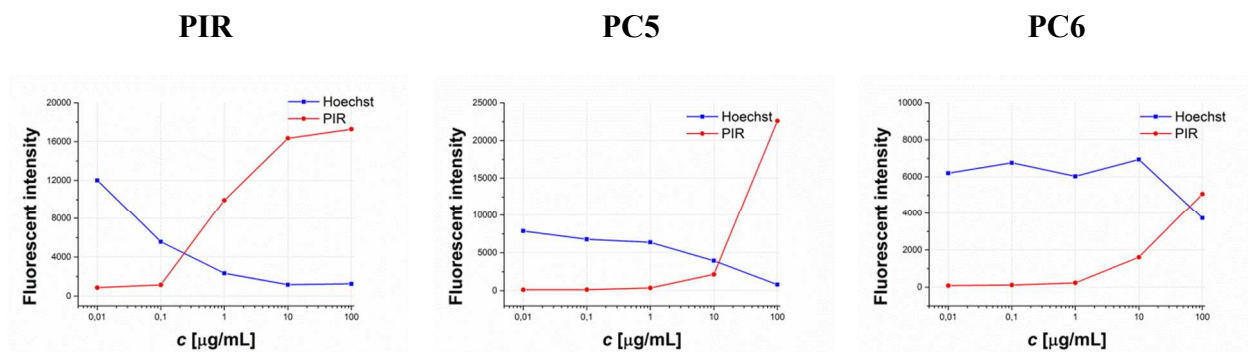
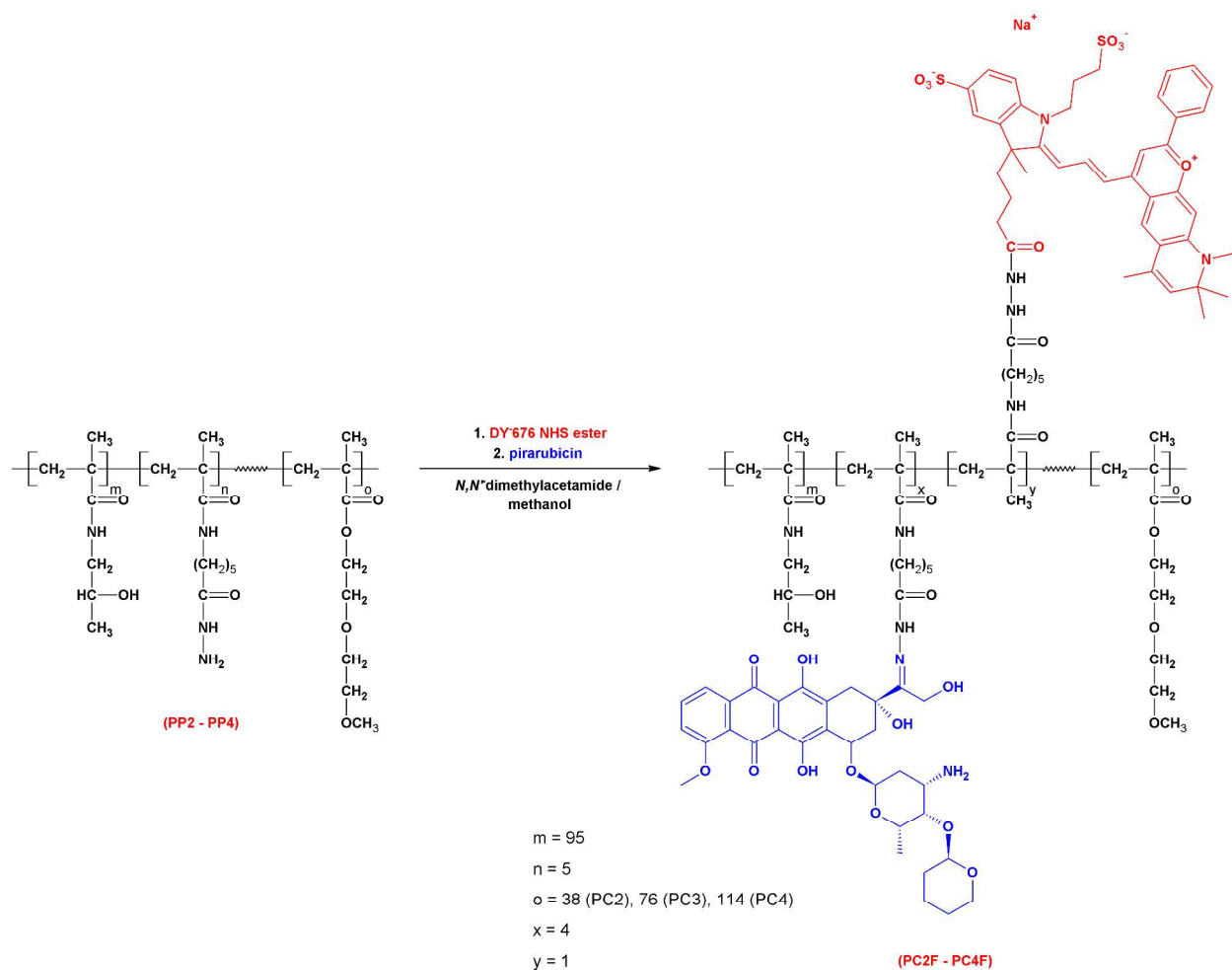


Figure 6. Incorporation of PIR released from the polymer-PIR conjugates into the DLD-1 cell nuclei evaluated from the decrease of the fluorescence intensity of Hoechst 333258 dye (blue line) or from the increase of the fluorescence intensity of PIR (red line), respectively, as a result of the intercalation competition between PIR and Hoechst 333258 dye.



Scheme 2. Conjugation of pirarubicin and DY-676 fluorescent dye with di-block copolymer precursors **PP2 – PP4** through the hydrazone and diacylhydrazine bond, respectively.

Conjugates **PC2 – PC4** were prepared analogously in absence of DY-676.

Tables

Table 1. Molecular weight parameters of the copolymer precursors **PP1 – PP4** obtained from SEC analysis.

Polymer precursor	Structure	ⁱ [PP1] / [DEGMA]	ⁱⁱ M_n [g/mol]	ⁱⁱⁱ \bar{D}	T_{tr} [°C]
-------------------	-----------	------------------------------	-----------------------------	--------------------------	---------------

PP1	p[(HPMA)- <i>co</i> -(Ma-Ahx-NHNH-Boc)]	-	14,100	1.11	-
PP2	p[(HPMA)- <i>co</i> -(Ma-Ahx-NHNH ₂)]- <i>b</i> -p(DEGMA)	1 / 38	21,100	1.55	44
PP3	p[(HPMA)- <i>co</i> -(Ma-Ahx-NHNH ₂)]- <i>b</i> -p(DEGMA)	1 / 76	31,000	1.47	33
PP4	p[(HPMA)- <i>co</i> -(Ma-Ahx-NHNH ₂)]- <i>b</i> -p(DEGMA)	1 / 114	38,700	1.51	31

ⁱMolar ratios of DTB-end groups of **PP1** precursor to DEGMA monomer in the polymerization feed.

ⁱⁱNumber-averaged molecular weights evaluated by GPC using the LS and RI detectors

ⁱⁱⁱPolydispersity indexes (ratios of weight- and number-averaged molecular weights)

Table 2. Physicochemical characteristics of the thermo-responsive polymer-PIR conjugates **PC2** – **PC4**.

Polymer conjugate	PC2	PC3	PC4
Polymer precursor	PP2	PP3	PP4
ⁱ M_n [g/mol]	21,500	31,800	40,000
ⁱⁱ \mathcal{D}	1.43	1.47	1.46
ⁱⁱⁱ ω^{PIR} [wt. %]	7.9	7.3	7.3
^{iv} D_H^{rc} [nm] ($T < T_{tr}$)	8.4	8.9	10.6
^v D_H^{mic} [nm] ($T > T_{tr}$)	31.5	37.3	50.0
T_{tr} [°C]	39	30	26
CMC [mg/mL]	0.071	0.053	0.022

ⁱNumber-averaged molecular weights evaluated by SEC using a relative calibration

ⁱⁱPolydispersity indexes (ratios of weight- and number-averaged molecular weights)

ⁱⁱⁱWeight contents of PIR in polymer-PIR conjugates

^{iv}Hydrodynamic diameters of polymer-PIR conjugate particles (polymer micelles) below the transition temperature

^vHydrodynamic diameters of polymer-PIR conjugate particles (unimers) above the transition temperature

Table 3. IC₅₀ values for the polymer-PIR conjugates and free PIR measured on DLD-1 and EL-4 cell lines using the cell viability assay.

Sample	IC ₅₀ [μg/mL]	
	DLD-1	EL-4
PC2	3.26	0.0118
PC3	2.92	0.0153
PC4	3.11	0.0120
PIR	0.16	>0.0001
ⁱ PC5	1.41	0.0004
PC6	16.45	n.d.

ⁱConjugate of hydrophilic p[(HPMA)-*co*-(Ma-Ahx-NHNH₂)] polymer precursor with PIR bound to the polymer backbone through the hydrolytically degradable hydrazone bond (*M*_w = 36,800 g/mol, *M*_w/*M*_n = 1.92, ω^{PIR} = 8.9 wt. %) prepared as described³⁶. For the structure, see Figure S1 A.

Supporting Information

The document shows chemical structures of the polymer conjugates **PC5** and **PC6**, examples of the detailed SEC profiles for the polymers **PP2** and **PC2** and comparison of the temperature dependences of the polymer conjugate **PC2** before and after hydrolysis. This material is available at free of charge via the Internet at <http://pubs.acs.org>.

Corresponding Author

*(R.L.) E.mail: laga@imc.cas.cz

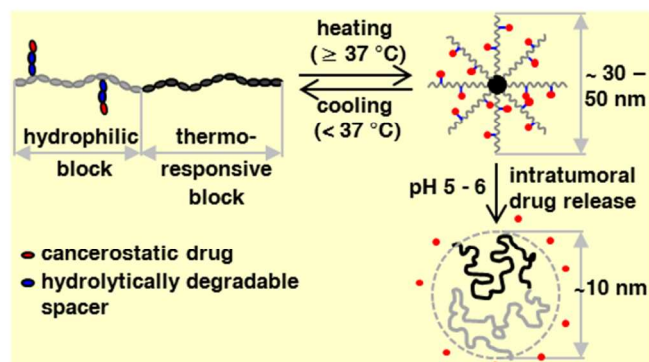
Author Contributions

The manuscript was written through contributions of all authors. All authors have given approval to the final version of the manuscript.

Acknowledgement

This work was financially supported by a grant of Ministry of Education, Youth and Sports of the Czech Republic (grant No. EE2.3.30.0029) and by BIOCEV (CZ.1.05/1.1.00/02.0109) - Biotechnology and Biomedicine Centre of the Academy of Sciences and Charles University from the European Regional Development Fund.

Table of Contents



References

1. Hill, A. V.; Reyes-Sandoval, A.; O'Hara, G.; Ewer, K.; Lawrie, A.; Goodman, A.; Nicosia, A.; Folgori, A.; Colloca, S.; Cortese, R.; Gilbert, S. C.; Draper, S. J., Prime-boost vectored malaria vaccines: progress and prospects. *Human vaccines* **2010**, 6, (1), 78-83.
2. Satchi-Fainaro, R.; Duncan, R.; Barnes, C. M., Polymer therapeutics for cancer: Current status and future challenges. *Adv Polym Sci* **2006**, 193, 1-65.
3. Matsumura, Y.; Maeda, H., A New Concept for Macromolecular Therapeutics in Cancer-Chemotherapy - Mechanism of Tumoritropic Accumulation of Proteins and the Antitumor Agent Smancs. *Cancer Res* **1986**, 46, (12), 6387-6392.
4. Maeda, H., Macromolecular therapeutics in cancer treatment: The EPR effect and beyond. *J Control Release* **2012**, 164, (2), 138-144.
5. Maeda, H.; Nakamura, H.; Fang, J., The EPR effect for macromolecular drug delivery to solid tumors: Improvement of tumor uptake, lowering of systemic toxicity, and distinct tumor imaging in vivo. *Adv Drug Deliver Rev* **2013**, 65, (1), 71-79.
6. Etrych, T.; Jelinkova, M.; Rihova, B.; Ulbrich, K., New HPMA copolymers containing doxorubicin bound via pH-sensitive linkage: synthesis and preliminary in vitro and in vivo biological properties. *J Control Release* **2001**, 73, (1), 89-102.
7. Rejmanova, P.; Kopecek, J.; Pohl, J.; Baudys, M.; Kostka, V., Polymers Containing Enzymatically Degradable Bonds .8. Degradation of Oligopeptide Sequences in N-(2-Hydroxypropyl)Methacrylamide Co-Polymers by Bovine Spleen Cathepsin-B. *Makromol Chem* **1983**, 184, (10), 2009-2020.
8. Shen, W. C.; Ryser, H. J. P., Cis-Aconityl Spacer between Daunomycin and Macromolecular Carriers - a Model of Ph-Sensitive Linkage Releasing Drug from a Lysosomotropic Conjugate. *Biochem Bioph Res Co* **1981**, 102, (3), 1048-1054.
9. Etrych, T.; Subr, V.; Strohalm, J.; Sirova, M.; Rihova, B.; Ulbrich, K., HPMA copolymer-doxorubicin conjugates: The effects of molecular weight and architecture on

1
2
3 biodistribution and in vivo activity. *Journal of controlled release : official journal of the*
4 *Controlled Release Society* **2012**, 164, (3), 346-54.

7
8 10. Etrych, T.; Kovar, L.; Strohalm, J.; Chytil, P.; Rihova, B.; Ulbrich, K., Biodegradable star
9 HPMA polymer-drug conjugates: Biodegradability, distribution and anti-tumor efficacy. *J*
10 *Control Release* **2011**, 154, (3), 241-248.

13
14 11. Filippov, S. K.; Chytil, P.; Konarev, P. V.; Dyakonova, M.; Papadakis, C. M.; Zhigunov,
15 A.; Plestil, J.; Stepanek, P.; Etrych, T.; Ulbrich, K.; Svergun, D. I., Macromolecular HPMA-
16 Based Nanoparticles with Cholesterol for Solid-Tumor Targeting: Detailed Study of the Inner
17 Structure of a Highly Efficient Drug Delivery System. *Biomacromolecules* **2012**, 13, (8), 2594-
18 2604.

21
22 23
24 12. Liu, R.; Li, D.; He, B.; Xu, X. H.; Sheng, M. M.; Lai, Y. S.; Wang, G.; Gu, Z. W., Anti-
25 tumor drug delivery of pH-sensitive poly(ethylene glycol)-poly(L-histidine)-poly(L-lactide)
26 nanoparticles. *J Control Release* **2011**, 152, (1), 49-56.

29
30 31 13. Thambi, T.; Yoon, H. Y.; Kim, K.; Kwon, I. C.; Yoo, C. K.; Park, J. H., Bioreducible
32 Block Copolymers Based on Poly(Ethylene Glycol) and Poly(gamma-Benzyl L-Glutamate) for
33 Intracellular Delivery of Camptothecin. *Bioconjugate Chem* **2011**, 22, (10), 1924-1931.

36
37 14. Batrakova, E. V.; Kabanov, A. V., Pluronic block copolymers: Evolution of drug delivery
38 concept from inert nanocarriers to biological response modifiers. *J Control Release* **2008**, 130,
39 (2), 98-106.

42
43 15. Meyer, D. E.; Shin, B. C.; Kong, G. A.; Dewhirst, M. W.; Chilkoti, A., Drug targeting
44 using thermally responsive polymers and local hyperthermia. *J Control Release* **2001**, 74, (1-3),
45 213-224.

48
49 16. Hruby, M.; Konak, C.; Kucka, J.; Vetrik, M.; Filippov, S. K.; Vetvicka, D.; Mackova, H.;
50 Karlsson, G.; Edwards, K.; Rihova, B.; Ulbrich, K., Thermoresponsive, Hydrolytically
51 Degradable Polymer Micelles Intended for Radionuclide Delivery. *Macromol Biosci* **2009**, 9,
52 (10), 1016-1027.

1
2
3 17. Hoogenboom, R.; Thijs, H. M. L.; Jochems, M. J. H. C.; van Lankvelt, B. M.; Fijten, M.
4 W. M.; Schubert, U. S., Tuning the LCST of poly(2-oxazoline)s by varying composition and
5 molecular weight: alternatives to poly(N-isopropylacrylamide)? *Chem Commun* **2008**, (44),
6 5758-5760.
7
8

9
10
11 18. Bogomolova, A.; Filippov, S. K.; Starovoytova, L.; Angelov, B.; Konarev, P.; Sedlacek,
12 O.; Hruby, M.; Stepanek, P., Study of Complex Thermosensitive Amphiphilic Polyoxazolines
13 and Their Interaction with Ionic Surfactants. Are Hydrophobic, Thermosensitive, and
14 Hydrophilic Moieties Equally Important? *J Phys Chem B* **2014**, 118, (18), 4940-4950.
15
16

17
18
19 19. Fernandez-Trillo, F.; Dureault, A.; Bayley, J. P. M.; van Hest, J. C. M.; Thies, J. C.;
20 Michon, T.; Weberskirch, R.; Cameron, N. R., Elastin-based side-chain polymers: Improved
21 synthesis via RAFT and stimulus responsive behavior. *Macromolecules* **2007**, 40, (17), 6094-
22 6099.
23
24

25
26
27 20. Lutz, J. F.; Akdemir, O.; Hoth, A., Point by point comparison of two thermosensitive
28 polymers exhibiting a similar LCST: Is the age of poly(NIPAM) over? *J Am Chem Soc* **2006**,
29 128, (40), 13046-13047.
30
31

32
33
34 21. Conrad, R. M.; Grubbs, R. H., Tunable, Temperature-Responsive Polynorbornenes with
35 Side Chains Based on an Elastin Peptide Sequence. *Angew Chem Int Edit* **2009**, 48, (44), 8328-
36 8330.
37
38

39
40
41 22. Becer, C. R.; Hahn, S.; Fijten, M. W. M.; Thijs, H. M. L.; Hoogenboom, R.; Schubert, U.
42 S., Libraries of Methacrylic Acid and Oligo(ethylene glycol) Methacrylate Copolymers with
43 LCST Behavior. *J Polym Sci Pol Chem* **2008**, 46, (21), 7138-7147.
44
45

46
47 23. Bebis, K.; Jones, M. W.; Haddleton, D. M.; Gibson, M. I., Thermoresponsive behaviour
48 of poly[(oligo(ethyleneglycol methacrylate)]s and their protein conjugates: importance of
49 concentration and solvent system. *Polym Chem-Uk* **2011**, 2, (4), 975-982.
50
51

52
53 24. Pechar, M.; Pola, R.; Laga, R.; Braunova, A.; Filippov, S. K.; Bogomolova, A.;
54 Bednarova, L.; Vanek, O.; Ulbrich, K., Coiled Coil Peptides and Polymer-Peptide Conjugates:
55
56

1
2
3
4
5
6
7
8
9
10
11
12
13
14
15
16
17
18
19
20
21
22
23
24
25
26
27
28
29
30
31
32
33
34
35
36
37
38
39
40
41
42
43
44
45
46
47
48
49
50
51
52
53
54
55
56
57
58
59
60

Synthesis, Self-Assembly, Characterization and Potential in Drug Delivery Systems. *Biomacromolecules* **2014**, 15, (7), 2590-2599.

25. Carlisle, R.; Choi, J.; Bazan-Peregrino, M.; Laga, R.; Subr, V.; Kostka, L.; Ulbrich, K.; Coussios, C. C.; Seymour, L. W., Enhanced Tumor Uptake and Penetration of Virotherapy Using Polymer Stealthing and Focused Ultrasound. *Jnci-J Natl Cancer I* **2013**, 105, (22), 1701-1710.

26. Sirova, M.; Kabesova, M.; Kovar, L.; Etrych, T.; Strohalm, J.; Ulbrich, K.; Rihova, B., HPMA Copolymer-Bound Doxorubicin Induces Immunogenic Tumor Cell Death. *Curr Med Chem* **2013**, 20, (38), 4815-4826.

27. Etrych, T.; Mrkvan, T.; Chytil, P.; Konak, C.; Rihova, B.; Ulbrich, K., N-(2-hydroxypropyl)methacrylamide-based polymer conjugates with pH-controlled activation of doxorubicin. I. New synthesis, physicochemical characterization and preliminary biological evaluation. *J Appl Polym Sci* **2008**, 109, (5), 3050-3061.

28. Ulbrich, K.; Subr, V.; Strohalm, J.; Plocova, D.; Jelinkova, M.; Rihova, B., Polymeric drugs based on conjugates of synthetic and natural macromolecules I. Synthesis and physicochemical characterisation. *J Control Release* **2000**, 64, (1-3), 63-79.

29. Ulbrich, K.; Etrych, T.; Chytil, P.; Jelinkova, M.; Rihova, B., Antibody-targeted polymer-doxorubicin conjugates with pH-controlled activation. *J Drug Target* **2004**, 12, (8), 477-489.

30. Subr, V.; Ulbrich, K., Synthesis and properties of new N-(2-hydroxypropyl)-methacrylamide copolymers containing thiazolidine-2-thione reactive groups. *React Funct Polym* **2006**, 66, (12), 1525-1538.

31. Chytil, P.; Etrych, T.; Kriz, J.; Subr, V.; Ulbrich, K., N-(2-Hydroxypropyl)methacrylamide-based polymer conjugates with pH-controlled activation of doxorubicin for cell-specific or passive tumour targeting. Synthesis by RAFT polymerisation and physicochemical characterisation. *Eur J Pharm Sci* **2010**, 41, (3-4), 473-482.

32. Etrych, T.; Subr, V.; Laga, R.; Rihova, B.; Ulbrich, K., Polymer conjugates of doxorubicin bound through an amide and hydrazone bond: Impact of the carrier structure onto synergistic action in the treatment of solid tumours. *Eur J Pharm Sci* **2014**, 58, 1-12.

1
2
3 33. Nakamura, H.; Etrych, T.; Chytil, P.; Ohkubo, M.; Fang, J.; Ulbrich, K.; Maeda, H., Two
4 step mechanisms of tumor selective delivery of N-(2-hydroxypropyl) methacrylamide copolymer
5 conjugated with pirarubicin via an acid-cleavable linkage. *Journal of Controlled Release* **2014**,
6 174, 81-87.
7
8
9

10
11 34. Hovorka, O.; St'astny, M.; Etrych, T.; Subr, V.; Strohalm, J.; Ulbrich, K.; Rihova, B.,
12 Differences in the intracellular fate of free and polymer-bound doxorubicin. *Journal of*
13 *Controlled Release* **2002**, 80, (1-3), 101-117.
14
15
16

17
18 35. Hovorka, O.; Subr, V.; Vetvicka, D.; Kovar, L.; Strohalm, J.; Strohalm, M.; Benda, A.;
19 Hof, M.; Ulbrich, K.; Rihova, B., Spectral analysis of doxorubicin accumulation and the indirect
20 quantification of its DNA intercalation. *Eur J Pharm Biopharm* **2010**, 76, (3), 514-524.
21
22
23

24 36. Nakamura, H.; Etrych, T.; Chytil, P.; Ohkubo, M.; Fang, J.; Ulbrich, K.; Maeda, H., Two
25 step mechanisms of tumor selective delivery of N-(2-hydroxypropyl) methacrylamide copolymer
26 conjugated with pirarubicin via an acid-cleavable linkage (vol 174, pg 81, 2014). *J Control*
27 *Release* **2014**, 182, 97-98.
28
29
30

31
32 37. Weerasinghe, P.; Buja, L. M., Oncosis: An important non-apoptotic mode of cell death.
33 *Exp Mol Pathol* **2012**, 93, (3), 302-308.
34
35
36
37
38
39
40
41
42
43
44
45
46
47
48
49
50
51
52
53
54
55
56
57
58
59
60